Experimental Investigation on Temperature Dependence of the Performance in a Magnetostrictive Fiber-Optic Interferometric Magnetic Field Sensor

Xin Wang, Xinwan Li, *Senior Member, IEEE*, Zhigang Du, Xiaoyang Wang, and Jianping Chen

***Abstract*—This paper studies the temperature dependence of the performance in magnetostrictive fiber-optic Michelson interferometric magnetic field sensors. Experiments are carried out and the results show that the sensor system output, system sensitivity and transducer's mechanical resonant frequency are strongly affected by the ambient temperature. Fitted expressions are provided and compensation methods are demonstrated with experimental verification.**

***Index Terms*—Fiber-optic interferometric magnetic field transducer, mechanical resonant frequency, system output, temperature behavior.**

I. Introduction

MUCH attention has been paid to magnetism-based sensors that can be widely used in measurement of physical [1]–[3], chemical, and even biological parameters [4], [5]. Magnetoelastic material, such as amorphous ferromagnetic alloy, is generally utilized as the sensing element in these sensors because of its excellent magnetic and physical properties, e.g. large magnetostriction, high magnetoelastic coupling, low coercivity, and etc. [6]–[8]. As a branch of magnetism-based sensors, the fiber-optic magnetic field sensor based on magnetostrictive effect shows many advantages in comparison with traditional methods, such as high sensitivity, electromagnetic immunity and so on, in detecting weak magnetic fields, especially DC or slowly varying ones [9]–[11]. A minimum detectable field of $11 \pm 2\ \mathrm{pT/Hz^{1/2}}$ at 1 Hz was demonstrated by Naval Research Lab, USA [12]. Mach-Zehnder or Michelson fiber-optic interferometric configurations are usually employed [12]–[14]. The sensing fiber and magnetostrictive material are bonded together as the transducer [15]. When DC or slowly varying magnetic field to be detected is applied along with an AC dither field on the transducer, the magnetostrictive material produces a magnetic-field-dependent strain, which introduces fiber length change, or actually phase change to the light propagating in the sensing fiber. By detecting the phase change, the magnetic field can be obtained.

The employment of an AC dither field is the simplest and the most convenient way to improve the performance of the magnetic field transducer in detecting DC or slowly varying magnetic field at present for it can overcome the $1/f$ noise [16]. Moreover, by tuning the dithering frequency in consistent with the peak mechanical resonant frequency of the transducer, it arouses the magnetoelastic resonance of the transducer and makes the sensor work at more sensitive status [17]. The magnetoelastic resonant frequency depends strongly on the ambient temperature and the dependence could lead to the decay of the sensor system output according to our studies. Thus, it is necessary to study the temperature dependence. Up to date, studies have been carried out on the temperature response in magnetoelastic sensors [5], [18]. However, the temperature behavior of fiber-optic interferometer-based magnetic field sensors still needs further investigation. Unfortunately, it is difficult to establish a precise theoretical model to evaluate the temperature dependence. In this paper, we qualitatively analyze the factors that are responsible for the temperature dependence, and investigate experimentally the temperature behavior of the transducer's magnetoelastic resonance and the system output in a particular magnetostrictive fiber-optic interferometric magnetic field sensor. Temperature variation induced change in the transducer dimensions is found to have a significant influence on the transducer resonance. Experiential expressions are presented for developing temperature immunity or compensation technique.

II. Principle and Theoretic Analysis

The sensor we used in the experiment is a fiber-optic Michelson interferometric magnetic field sensor implemented in [19], as shown in Fig. 1. The sensing fiber and reference fiber are wound and bonded on the magnetostrictive material and the piezoelectric transducer (PZT), respectively. The magnetostrictive material is a kind of nonstandard Fe-Ni-base amorphous ferromagnetic alloy ribbon developed for scientific research purpose, whose performance is similar to Metglas 2826 MB. The employment of 45° Faraday rotator mirrors (FRMs) alleviates the perturbation of the state of polarization [13], while the optical circulator and isolators effectively overcome the Rayleigh backscattering [20]. The circulator can also provide the orthogonal output signal for differential detection. The system output at the quadrature state can be expressed as

$$V_o \propto G(H_d + H_{\mathrm{bias}})h \tag{1}$$

Manuscript received December 19, 2008; accepted May 28, 2009. Current version published September 02, 2009. This work was supported in part by the National Science Foundation of China (NSFC ID 90704002 and 60377013), in part by 863 Project (ID 2006AA01Z242 and 2007AA01Z275), in part by the Dawn Program for Excellent Scholars of Shanghai Municipal Education Commission, in part by the Program for New Century Excellent Talents in University of Ministry of Education of China, and in part by the Key Disciplinary Development Program of Shanghai (T0102). The associate editor coordinating the review of this paper and approving it for publication was Dr. Patrick Ruther.

The authors are with the State Key Laboratory of Advanced Optical Communication Systems and Networks, SEIEE Buildings, Shanghai Jiao Tong University, Shanghai 200240, China (e-mail: jpchen62@sjtu.edu.cn).

Digital Object Identifier 10.1109/JSEN.2009.2029813

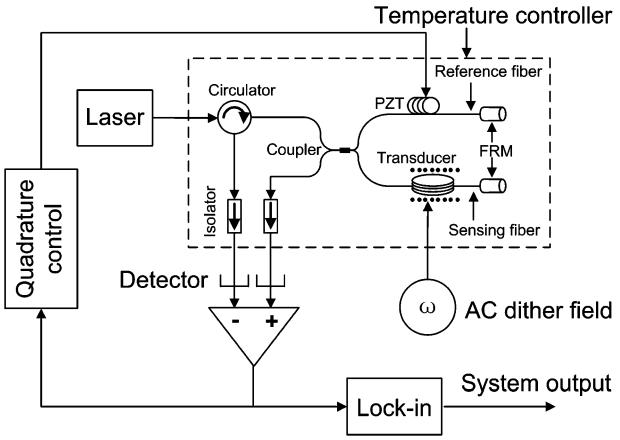

Fig. 1. Schematic diagram of magnetostrictive fiber-optic Michelson interferometric magnetic field sensor and experimental setup.

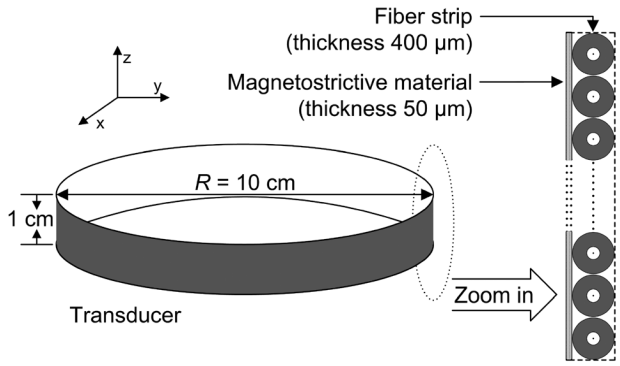

Fig. 2. Tridimensional configuration and a section of a magnetostrictive fiber-optic magnetic field transducer.

where G is a coefficient decided by the magnetostrictive material, transducing efficiency of the transducer and the gain of the detection circuit. It is also dependent on the system magnetoelastic resonance. H_d, $H_{\rm bias}$, and h are the magnetic field to be detected, the DC bias magnetic field and the AC dither field, respectively. GH_dh is the system output response induced by H_d.

Magnetoelastic resonance can be explained by elastic wave theory. Standing waves are produced because of the constant reflection and interference of a series of elastic waves propagating in a mechanical system exposed to a periodic force. The system will be at the resonant status and maintain that status once the frequency of the standing wave is equal or very close to the natural frequency of the system. For a ribbon-like mechanical system formed merely by single elastic material, its fundamental mechanical resonant frequency can be expressed as [21]

$$f = \frac{1}{2l}\left(\frac{E}{\rho}\right)^{1/2} \tag{2}$$

where l is the length of the mechanical system. E and ρ are the Young's modulus and the bulk density of the elastic medium, respectively. The change in l, E, and ρ will result in the shift of mechanical resonant frequency.

Fig. 2 shows the tridimensional configuration and a section of a cylindrical magnetostrictive fiber-optic magnetic field transducer. The fiber-optic transducer is a complex mechanical system. It consists of magnetostrictive material and optical fiber, which are in general bonded together. They have different Young's modulus and bulk density. Their interaction usually induces a series of subordinate resonant peaks in addition to the main resonant one. It is well-known that l, E, and ρ are more or less influenced by the temperature. Suppose a ribbon-like magnetostrictive fiber-optic magnetic field transducer of length L is fabricated and has a cross section as the cylindrical one shown in Fig. 2, its mechanical resonant frequency under the biasing of a constant external DC magnetic field, $H_{\rm dc}$, can be obtained through modifying (2) as [22]

$$f_{M-F} = \frac{1}{2L}\left(\frac{E_{\rm eff}}{\rho_{\rm eff}}\right)^{1/2} \times \left[1 + \frac{9E_{\rm eff}\lambda_s M^2(H)}{M_s^4}\frac{\partial M(H)}{\partial H}\right]^{-1/2}\Bigg|_{H=H_{\rm dc}} \tag{3}$$

where $\rho_{\rm eff}$, $E_{\rm eff}$ and λ_s are the mechanical parameters of the ribbon-like transducer ($\rho_{\rm eff}$: the effective bulk density, $E_{\rm eff}$: the effective Young's modulus, λ_s: the saturation magnetostriction), while M, M_s, and $\partial M/\partial H$ are the magnetic-related parameters of the magnetostrictive material (M: the magnetization, M_s: the saturation magnetization, $\partial M/\partial H$: the differential susceptibility). $E_{\rm eff}$ (or $\rho_{\rm eff}$) is decided by Young's modulus (or the bulk densities) and the cross section areas of the magnetostrictive material and fiber strip [23]. All the above parameters are assumed to be pure functions of temperature and different thermal expansion coefficients under the biasing of a constant external DC magnetic field. The changes in these parameters induced by the temperature variation will result in the shifts of mechanical resonant frequency. Hence, the mechanical resonant frequency of the ribbon-like transducer as a function of the temperature can be analyzed by replacing the parameters in (3) with their linear temperature dependences. Using the room temperature values of the parameters given in Table I along with their linear thermal expansion coefficients

TABLE I
ROOM TEMPERATURE PROPERTIES OF MAGNETOSTRICTIVE MATERIAL AND FIBER

	Parameters		Value at room temperature
Fiber [24], [25]	Dimensions (diameter μm)	Core	9
		Cladding	125
		Buffer coating	400
	Modulus* (GPa)		40
	Density* (kg/m^3)		1900
Magnetostrictive material [22]	Dimensions (μm)	Width	10^4
		Thickness	50
	Modulus (GPa)		110
	Density (kg/m^3)		7900
	λ_s(ppm)		12
	M_s(Tesla)		0.88
	M, $\frac{\partial M}{\partial H}$		Calculate from M-H curve

*The approximate effective modulus and density for the combination of the glass portion (core and cladding) and the buffer coating of the fiber.

TABLE II
THERMAL EXPANSION COEFFICIENTS FOR MAGNETOSTRICTIVE MATERIAL AND FIBER

	Parameters		Linear thermal expansion coefficient (ppm/℃)
Fiber[24], [25]	Dimensions (diameter μm)	Core & Cladding	0.5
		Buffer coating	200
	Modulus		128
Magnetostrictive material [22]	Dimensions		12
	Modulus		130
	λ_s		2800
	M_S, M, $\frac{\partial M}{\partial H}$		500

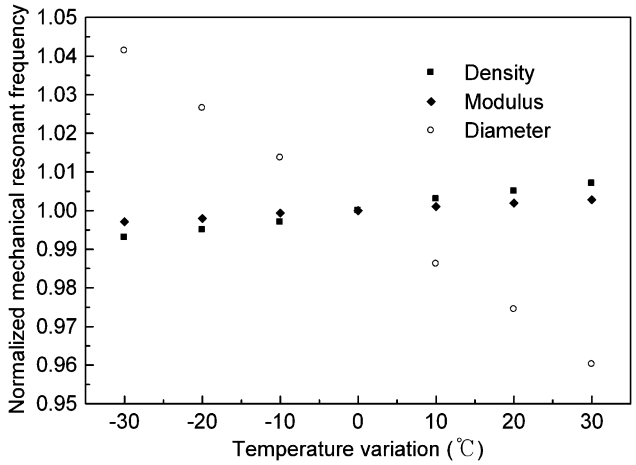

Fig. 3. Finite-element modality analysis result of the effects of thermal expansion in Young's modulus E_{eff}, density ρ_{eff}, and diameter R on mechanical resonant frequency around room temperature. Frequencies are normalized to the room temperature value. Temperature dependences of E_{eff}, ρ_{eff}, and R are supposed to be $D(\mathrm{T}) = D_0 + \alpha D_0 \Delta \mathrm{T}$ (D_0: room temperature value, α: thermal expansion coefficient, ΔT: temperature variation). Calculated E_{eff}, ρ_{eff} at room temperature and corresponding approximate thermal expansion coefficients: 50 GPa, 2600 $\mathrm{kg/m^3}$ and 120 $\mathrm{ppm/^\circ C}$, 400 $\mathrm{ppm/^\circ C}$, R, and its calculated thermal expansion coefficient: 10 cm and 150 $\mathrm{ppm/^\circ C}$.

given in Table II, the temperature dependence of the mechanical resonance can be obtained.

However, the magnetostrictive material in multilayer structure and cylindrical configuration is generally adopted in a real magnetostrictive fiber-optic interferometric magnetic field transducer [19], [26]. Thus, it is not easy to evolve an exact and simple expression as the one shown in (3) for a real transducer, especially to include the thermal expansion coefficients of all the parameters along with the size and shape of the transducer. Among the dimensions, Young's modulus and density parameters, it is found with the help of finite-element modality analysis (Fig. 3) that the change in the diameter R of the cylindrical transducer (as shown in Fig. 2) due to the temperature variation has a much stronger effect on the mechanical resonant frequency than the changes in Young's modulus and density. The change in the diameter R could attribute to the temperature induced thermal expansion in the dimensions of the silicone buffer coating of the fiber because that thermal expansion

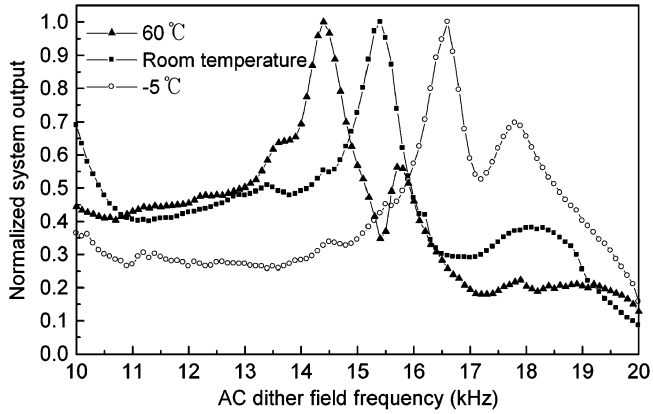

Fig. 4. System output as a function of AC dither field frequency under different ambient temperatures.

coefficient of the buffer coating is much larger than that of the core and cladding of the fiber and the magnetostrictive material.

III. EXPERIMENTAL RESULTS

We carried out experiments to characterize the real transducer's temperature behavior. The experimental setup is shown in Fig. 1. During the measurements, no mumetal shield was employed. The geomagnetic field, which can be considered a constant DC field, was used as the bias (H_{bias}) for this magnetostrictive fiber-optic interferometric magnetic field senor is designed to detect the geomagnetic field vibrations induced by magnetic objects.

A. Mechanical Resonant Frequency and System Output

At first, experiment was performed to study the temperature influence on the mechanical resonant frequency of the transducer. Fig. 4 shows the normalized frequency responses of the transducer as a function of AC dither field frequency at three different temperatures. It can be observed that the dither field frequency has a remarkable impact on system output meanwhile the ambient temperature variation does introduce shift to the mechanical resonant frequency. The output reaches the maximum at about 16.6, 15.5, and 14.4 kHz at -5 °C, room temperature and 60 °C, respectively. Fig. 5 shows mechanical resonant frequency drift as a function of the ambient temperature (left vertical ordinate). The drift can be expressed as a function of ambient temperature approximately

$$f_T = 15.5 + 1.29 \times 10^{-5}(T - 26.7)^3 - 4.73 \times 10^{-2}(T - 26.7)\mathrm{kHz} \quad (4)$$

where 26.7 is the room temperature in degree centigrade.

The system output was measured for different temperatures ranging from -5 °C to 60 °C. The AC dither field was tuned at the mechanical resonant frequency of the transducer at room temperature (15.5 kHz) and kept unchanged during the test. Each temperature was maintained for 2 h in order to let the system become stable [19] before measurement was performed. The normalized system output as a function of the ambient temperature is shown in Fig. 5 (right vertical ordinate). From Fig. 5, it can be seen that the ambient temperature has a strong impact

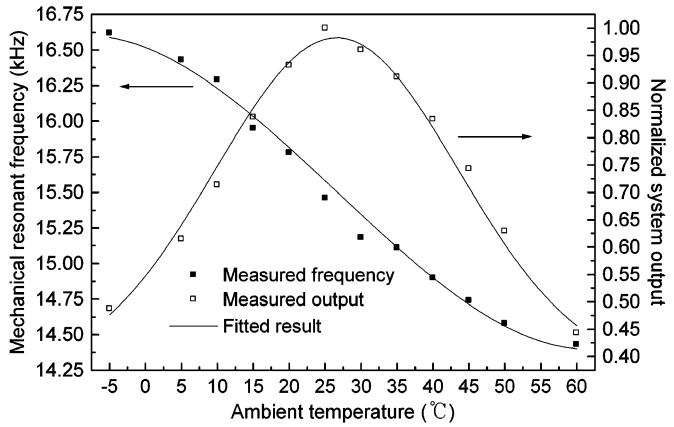

Fig. 5. Transducer's peak mechanical resonant frequency and system output as a function of ambient temperature.

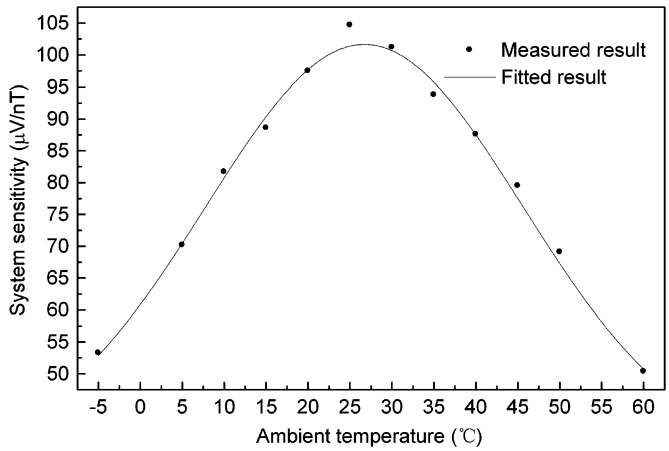

Fig. 6. System sensitivity as a function of ambient temperature.

on the sensor system output. The fitted curve indicates that the sensor system output and the ambient temperature closely correspond to a bell-shaped curve like the Gaussian distribution function, which can be expressed as

$$\bar{V}_{\mathrm{o}} = 0.37 + 0.61e^{-1.75\times10^{-3}(T-26.7)^2}. \tag{5}$$

B. System Sensitivity

In order to analyze the system sensitivity dependence on the ambient temperature, the AC dither field remained at 15.5 kHz. The system sensitivity (in $\mu\mathrm{V/nT}$, system output response leaded by a DC magnetic field of one nanotesla) was calculated from the system output response versus the measured DC magnetic field. Fig. 6 shows the system sensitivity as a function of the ambient temperature. It can be observed that the influence of the ambient temperature on the system sensitivity approximates to that of the ambient temperature on the system output. A decline in the system output is usually accompanied by a consequent decline in the system sensitivity. The system sensitivity can be formulized as

$$S_T = 105.9 \cdot \left[0.35 + 0.62e^{-1.40\times10^{-3}(T-26.7)^2}\right] \mu\mathrm{V/nT} \tag{6}$$

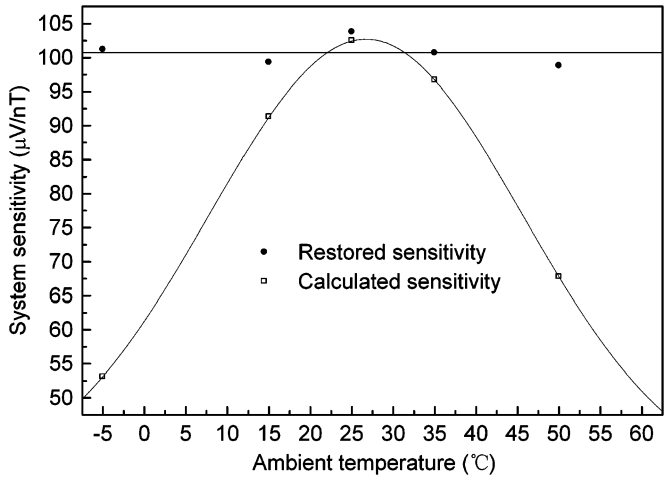

Fig. 7. Restored and calculated system sensitivities at different temperatures.

where 105.9 $\mu\mathrm{V/nT}$ is the system sensitivity at room temperature.

Though the exact temperature dependence of the transducer may change from one to another, the trend is almost the same. The optical phase drifts in the fiber-optic Michelson interferometric fibers due to the fiber length changes will not significantly discount the interferometric performance and then cause the system output to drop seriously because of the differential detection as well as the strictly controlled length difference (within 0.5 mm), which makes the two interferometric fibers have almost the same temperature response. Thus, the temperature induced mechanical resonant frequency drifts should be responsible for the decay of the system output. With this understanding, temperature compensation can be employed to make the sensors work independent on the ambient temperature.

C. Elimination of Temperature Dependence

There are two ways to eliminate the temperature dependence. One is active and the other is passive.

The active compensation scheme is to tune the AC dither field frequency in accordance with the ambient temperature using (4) with the help of a temperature sensor. By the way, the system output as well as the system sensitivity can be somewhat restored. The AC dither field employed in the study is produced by a sinusoidal signal generating circuit, whose frequency is regulated by a voltage-controlled module based on ordinary variable resistors and can only be adjusted manually. By replacing the variable resistors with thermistors, the AC dither field frequency can alter with the temperature. Of course, it is necessary to experimentally obtain the target transducer's peak mechanical resonant frequencies at different ambient temperatures as the curve shown in Fig. 5 during the design. The magnetic field to be detected at a certain temperature can be obtained through dividing the system output response by the restored system sensitivity.

Passive temperature compensation is actually to modify the tested results in the way similar to temperature calibration [5]. In comparison with the active method, it is more convenient and generic to remove the temperature dependence. The first step is to determine how the ambient temperature affects the system

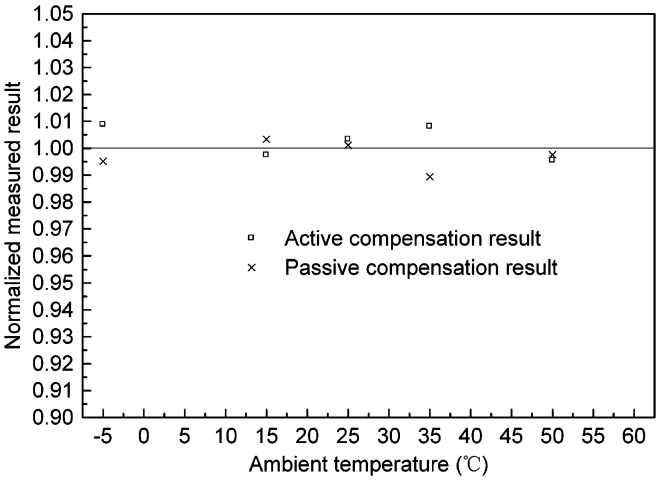

Fig. 8. Detection results with active and passive temperature compensation.

sensitivity, i.e., the sensitivity response to the ambient temperature, as shown in Fig. 6. The second step is to calculate the exact intensity of the field to be detected at a certain temperature according to the system output and the system sensitivity (the former being divided by the latter).

Experiments were performed to verify the feasibility of these two schemes. Fig. 7 shows the restored sensitivity (active compensation) and the calculated one (passive compensation), which is obtained by (6). It can be seen that the active method has evidently reduced the temperature dependence of the system sensitivity. The deviation mainly attributes to imperfectness of the dither generating circuit.

Fig. 8 shows the measured results of a known DC magnetic field at different temperatures using the above compensation methods. As can be seen temperature dependence has been effectively removed.

IV. Conclusion

The temperature behavior of fiber-optic interferometric magnetic field sensor based on magnetostrictive effect has been studied. The experimental results show that the ambient temperature can remarkably influence the transducer's mechanical resonant frequency and the system performance as well. Fitted expressions for temperature dependence are given. It is helpful to provide a guidance for the temperature immunity or compensation technique. Active and passive temperature compensation techniques are demonstrated. Experimental results show that they are practically applicable for magnetostrictive fiber-optic interferometric magnetic field sensors.

References

[1] J. M. Barandiaran and J. Gutierrez, "Magnetoelastic sensors based on soft amorphous magnetic alloys," *Sens. Actuators, A: Phys.*, vol. 59, no. 1–3, pp. 38–42, 1997.

[2] D. Kouzoudis and C. A. Grimes, "Remote query fluid-flow velocity measurement using magnetoelastic thick-film sensors (invited)," *J. Appl. Phys.*, vol. 87, no. 9 III, pp. 6301–6303, 2000.

[3] C. Petridis, A. Ktena, E. Laskaris, P. Dimitropoulos, and E. Hristoforou, "Ni-Fe thin film coated Cu wires for field sensing applications," *Sensor Lett.*, vol. 5, no. 1, pp. 93–97, 2007.

[4] T. Baimpos, I. G. Giannakopoulos, V. Nikolakis, and D. Kouzoudis, "Effect of gas adsorption on the elastic properties of faujasite films measured using magnetoelastic sensors," *Chem. Materials*, vol. 20, no. 4, pp. 1470–1475, 2008.

[5] K. G. Ong, E. L. Tan, C. A. Grimes, and R. Shao, "Removal of temperature and earth's field effects of a magnetoelastic pH sensor," *IEEE Sensors J.*, vol. 8, no. 4, pp. 341–346, Apr. 2008.

[6] A. Hernando, M. Vázquez, and J. M. Barandiarán, "Metallic glasses and sensing applications," *J. Phys. E: Scientific Instruments*, vol. 21, no. 12, pp. 1129–1139, 1988.

[7] K. G. Ong, M. K. Jain, C. Mungle, S. Schmidt, and C. A. Grimes, "Magnetism-based sensors," in *Proc. SPIE—Int. Soc. Opt. Eng.*, 2001, vol. 4467, pp. 158–172.

[8] E. Hristoforou and A. Ktena, "Magnetostriction and magnetostrictive materials for sensing applications," *J. Magn. Magn. Mater.*, vol. 316, no. 2, pp. 372–378, 2007.

[9] J. E. Lenz, "A review of magnetic sensors," *Proc. IEEE*, vol. 78, no. 6, pp. 973–989, 1990.

[10] L. L. Picon, V. M. Bright, and E. S. Kolesar, "Detecting low-intensity magnetic fields with a magnetostrictive fiber optic sensor," in *Proc. Aerosp. Electron. Conf., NAECON*, 1994, vol. 2, pp. 1034–1039.

[11] J. Lenz and S. Edelstein, "Magnetic sensors and their applications," *IEEE Sensors J.*, vol. 6, no. 3, pp. 631–649, Mar. 2006.

[12] D. M. Dagenais, F. Bucholtz, K. P. Koo, and A. Dandridge, "Detection of low-frequency magnetic signals in a magnetostrictive fiber-optic sensor with suppressed residual signal," *J. Lightw. Technol.*, vol. 7, no. 6, pp. 881–887, 1989.

[13] A. D. Kersey, M. J. Marrone, and M. A. Davis, "Polarisation-insensitive fibre optic Michelson interferometer," *Electron. Lett.*, vol. 27, no. 6, pp. 518–520, 1991.

[14] K. P. Koo, F. Bucholtz, D. M. Dagenais, and A. Dandridge, "A compact fiber-optic magnetometer employing an amorphous metal wire transducer," *IEEE Photon. Technol. Lett.*, vol. 1, no. 12, pp. 464–466, 1989.

[15] F. Bucholtz, K. P. Koo, J. G. H. Sigel, and A. Dandridge, "Optimization of the fiber/metallic glass bond in fiber-optic magnetic sensors," *J. Lightw. Technol.*, vol. 3, no. 4, pp. 814–817, 1985.

[16] K. P. Koo, A. Dandridge, A. Tveten, and G. Sigel, Jr., "A fiber-optic DC magnetometer," *J. Lightw. Technol.*, vol. 1, no. 3, pp. 524–525, 1983.

[17] D. M. Dagenais, F. Bucholtz, K. P. Koo, and A. Dandridge, "Demonstration of 3 $\mathrm{pT}/\mathrm{Hz}^{1/2}$ at 10 Hz in a fibre-optic magnetometer," *Electronics Lett.*, vol. 24, no. 23, pp. 1422–1423, 1988.

[18] K. G. Ong, C. S. Mungle, and C. A. Grimes, "Control of a magnetoelastic sensor temperature response by magnetic field tuning," *IEEE Trans. Magn.*, vol. 39, no. 5 II, pp. 3319–3321, 2003.

[19] X. Wang, S. Y. Chen, Z. G. Du, C. H. Shi, and J. P. Chen, "Experimental study of some key issues on fiber-optic interferometric sensors detecting weak magnetic field," *IEEE Sensors J.*, vol. 8, no. 7, pp. 1173–1179, 2008.

[20] M. J. Marrone, A. D. Kersey, C. A. Villarruel, C. K. Kirkendall, and A. Dandridge, "Elimination of coherent Rayleigh backscatter induced noise in fibre Michelson interferometers," *Electronics Lett.*, vol. 28, no. 19, pp. 1803–1804, 1992.

[21] L. Meirovitch, *Fundamentals of Vibrations*. New York: McGraw-Hill, 2001.

[22] C. Mungle, C. A. Grimes, and W. R. Dreschel, "Magnetic field tuning of the frequency-temperature response of a magnetoelastic sensor," *Sens. Actuators, A: Phys.*, vol. 101, no. 1–2, pp. 143–149, 2002.

[23] S. Schmidt and C. A. Grimes, "Elastic modulus measurement of thin films coated onto magnetoelastic ribbons," *IEEE Trans. Magn.*, vol. 37, no. 4 I, pp. 2731–2733, 2001.

[24] U. S. Raikar, A. S. Lalasangi, V. K. Kulkarni, and I. I. Pattanashetti, "Temperature dependence of bending loss in single mode communication fiber: Effect of fiber buffer coating," *Opt. Commun.*, vol. 273, no. 2, pp. 402–406, 2007.

[25] R. R. J. Maier, W. N. MacPherson, J. S. Barton, J. D. C. Jones, S. McCulloch, and G. Burnell, "Temperature dependence of the stress response of fibre Bragg gratings," *Measure. Sci. Technol.*, vol. 15, no. 8, pp. 1601–1606, 2004.

[26] C. H. Shi, J. P. Chen, G. L. Wu, X. W. Li, J. H. Zhou, and F. Ou, "Stable dynamic detection scheme for magnetostrictive fiber-optic interferometric sensors," *Opt. Express*, vol. 14, no. 12, pp. 5098–5102, 2006.

Xin Wang received the B.Sc. and M.Sc. degrees from Lanzhou University, Gansu, China, in 2002 and 2005, respectively. He is currently working towards the Ph.D. degree at the State Key Laboratory of Advanced Optical Communication Systems and Networks, Shanghai Jiao Tong University, Shanghai, China.

His research interests focus on fiber-optic sensing and its signal processing.

Xinwan Li (SM'09) received the B.Sc. degree from Suzhou University, Suzhou, Jiangsu, China, in 1990, the M.Sc. degree from Shanghai University of Science and Technology (now named as Shanghai University), Shanghai, China, in 1993, and the Ph.D. degree from Shanghai Jiao Tong University, Shanghai, China, in 2005.

Since 1993, he has been working at the State Key Laboratory of Advanced Optical Communication Systems and Networks, Shanghai Jiao Tong University, Shanghai, China. He visited Essex University as a Research Attachment with Prof. M. O'Mahony during 1997–1998, as a Research Engineer at OPCOM, San Jose, CA for nine months in 2001, and a visiting Professor at Chonbuk National Univeristy for three month in 2007. From 2005, he has been a Professor at Shanghai Jiao Tong University. His main research includes fast optical switching devices, subsystems and networks, fiber-optic sensing and digital optical signal processing.

Zhigang Du, photograph and biography not available at the time of publication.

Xiaoyang Wang, photograph and biography not available at the time of publication.

Jianping Chen received the B.Sc. degree from Zhejiang University, Zhejiang, China, in 1983 and the M.Sc. and Ph.D. degrees from Shanghai Jiao Tong University, Shanghai, China, in 1986 and 1992, respectively.

Currently, he is a Professor at the State Key Laboratory of Advanced Optical Communication Systems and Networks, Shanghai Jiao Tong University, Shanghai, China. His main research areas cover photonic devices and subsystems, optical networks, fiber-optic sensing, and optical signal processing.